A STUDY OF HYDROGEN DIFFUSION FLAMES USING PDF TURBULENCE MODEL

Andrew T. Hsu*
Sverdrup Technology, Inc.
NASA Lewis Research Center, Cleveland, Ohio 44145

Abstract

The application of probability density function (pdf) turbulence models is addressed in this work. For the purpose of accurate prediction of turbulent combustion, an algorithm that combines a conventional CFD flow solver with the Monte Carlo simulation of the pdf evolution equation has been developed. The algorithm has been validated using experimental data for a heated turbulent plane jet. The study of H_2–F_2 diffusion flames has been carried out using this algorithm. Numerical results compared favorably with experimental data. The computations show that the flame center shifts as the equivalence ratio changes, and that for the same equivalence ratio, similarity solutions for flames exist.

Introduction

It is the consensus of the combustion profession that the prediction of chemical reaction rate (the source term in a species conservation equation) is poor if a conventional turbulence model is used. The main difficulty lies in the fact that the reaction rate is highly non-linear, and the use of averaged temperature, pressure and density produces excessively large errors. Moment closure models for the source terms have attained only limited success because the assumptions for such models to be valid often can not be satisfied. The probability density function (pdf) method seems to be the only alternative at the present time that uses local instantaneous values of the temperature, density, etc., in predicting the chemical reaction rate, and thus is the only viable approach for more accurate turbulent combustion calculations. Two main lines are being followed in pdf methods: one uses an assumed shape for the pdf, the second solves a pdf evolution equation; the present paper addresses only the latter. There has been significant progress in the study of pdf turbulence models in low speed flows in the past decades. These developments were summarized in Refs. [1], [2] and [3]. In spite of this progress, pdf turbulence modeling remains a nascent discipline with many unresolved issues.

The fact that the pdf equation has a very large dimensionality renders the use of finite difference schemes extremely demanding on computer memories and thus impractical, if not entirely impossible. A logical alternative is the Monte Carlo scheme, which has been used extensively in statistical physics. The evolution equations for the joint pdf of the velocity and species mass fraction have been successfully solved using Monte Carlo schemes, see, e.g., Pope[1]. However, since CFD has reached a certain degree of maturity as well as acceptance, it seems, at least from the standpoint of practical applications, that the use of a combined CFD and Monte Carlo scheme is more beneficial. Therefore, in the present study a scheme is chosen that uses a conventional CFD algorithm to solve the Navier-Stokes equations and provide flowfield properties such as velocity, pressure, etc., and the chemical reactions are calculated by using a Monte Carlo scheme to solve a pdf evolution equation.

The combined CFD-pdf solver has been developed recently and validated using non-reacting flow data for a heated turbulent plane jet. The algorithm has been further tested in the numerical study of an H_2–F_2 diffusion flame. This diffusion flame was studied experimentally by Mungal & Dimotakis[4] and Hermanson & Dimotakis[5]. The numerical results from the present study are compared with these experimental data.

Theory

Governing equations for reacting flows.

Flows with chemical reaction are governed by the continuity equation, momentum equations, energy equation, and species transport equations:

$$\begin{aligned}
&\partial_t \rho + \partial_i \rho u_i = 0 \\
&\rho \partial_t u_i + \rho u_j \partial_j u_i = -\partial_i p + \mu \partial_j \tau_{ij} \\
&\rho \partial_t h + \rho u_j \partial_j - \partial_t p - u_j \partial_j p \\
&\quad = -\partial_j q_j + Q \\
&\rho \partial_t Y_k + \rho u_j \partial_j Y_k = \rho \partial_j (D \partial_j Y_k) + w_k \\
&\quad k = 1, 2, \cdots, N.
\end{aligned} \tag{1}$$

where u_i is the velocity, Y_k is the mass fraction, and w_k is the chemical source term. (In addition to these equations, one also needs the equation of state.) For turbulent flows, we substitute

$$\begin{aligned}
u_i &= \tilde{u}_i + u_i', \\
Y_i &= \tilde{Y}_i + Y_i',
\end{aligned} \tag{2}$$

into the above equation and take an ensemble average. In the process of averaging, new unknown quantities in the form of correlations appear, e.g., $\overline{u_i' u_j'}$, $\overline{u_i' Y_k'}$, etc. These quantities can all be modeled using conventional turbulence models, such as two equation models or second order closure models. A problem unique to flows with chemical reaction is the average

of the chemical source term, $\overline{\rho w_k}$, The major difficulty lies in the fact that w_k is a highly nonlinear (usually exponential) function of the temperature. It is well know that the use of averaged temperature, $\tilde{T}$, in evaluating $\overline{\rho w_i}$ can cause egregious errors. One may consider the effect of the temperature fluctuation, T', by applying a moment closure model to the term $\overline{\rho w_i}$; however, such a closure model results in an infinite series that converges only when $T_a \sim \tilde{T}$ and $T' \ll \tilde{T}$. In many combustion problems, these two conditions are violated: in fact, we often have $T_a \gg \tilde{T}$ and $T' \sim \tilde{T}$ instead. In view of the above, the prospect of an accurate prediction of turbulent combustion using conventional turbulence models seems dismal. The above fact motivated the use of pdf methods.

Pdf evolution equation

Given a set of m random variables, $\psi_1, \psi_2, \cdots, \psi_m$, and the joint probability density function, $P(\psi_1, \psi_2, \cdots, \psi_m; x, y, z, t)$, the mean of any random function, $f(\psi_1, \psi_2, \cdots, \psi_m; x, y, z, t)$, can be calculated as

$$\overline{f(x,y,z,t)} = \int \cdots \int f\, P\, d\psi_1\, d\psi_2 \cdots d\psi_m. \quad (3)$$

For simple flows, one could assume the shape of the pdf and compute the source term, $\overline{\rho w_k}$, based on the assumed pdf using the above integral. For more general problems, one needs to solve a pdf evolution equation for a more accurate pdf distribution. In the latter case, the evaluation of the source term, $\overline{\rho w_k}$, is no longer necessary because the mean values of the temperature, species mass fractions, which we previously would obtain by solving the transport equations (Eq. 1), can now be evaluated directly from the pdf using the above integral.

The pdf evolution equation can be derived from the transport equations (Eq. 1) in many different ways, using a Dirac delta function, a characteristic function, or a characteristic functional. [1-3] The evolution equation of a single point probability density function of scalar random variables $\psi_1, \cdots, \psi_m$ can be written as

$$\begin{aligned} &\bar{\rho}\partial_t \tilde{P} + \bar{\rho}\tilde{v}_\alpha \partial_\alpha \tilde{P} + \bar{\rho}\sum_{i=1}^{m} \partial_{\psi_i}\{w_i(\psi_1, \cdots, \psi_m)\tilde{P}\} \\ &= -\partial_\alpha(\bar{\rho} < v''_\alpha | \phi_k(x) = \psi_k > \tilde{P}) \\ &\quad -\bar{\rho}\sum_{i=1}^{m}\sum_{j=1}^{m} \partial^2_{\psi_i,\psi_j}(< \epsilon_{ij} | \phi_k(x) = \psi_k > \tilde{P}) \end{aligned} \quad (4)$$

where the terms represent the rate of time change, mean convection, chemical reaction, turbulent convection, and molecular mixing, respectively; $\tilde{P}$ is the density-weighted joint pdf:

$$\tilde{P} = \rho P/\bar{\rho},$$

ϵ_{ij} is the scalar dissipation:

$$\epsilon_{ij} = D\partial_\alpha \phi_i \partial_\alpha \phi_j,$$

(where D is the diffusion coefficient), and $< x|y >$ denotes the mathematical expectation of a random function x conditioned upon y.

The left hand side of eq. (4) can be evaluated exactly and requires no modeling; the right hand side terms contain the conditional expectation of the velocity fluctuation and the conditional expectation of the scalar dissipation, which are new unknowns and require modeling.

Closure models for pdf equation

The first term that needs modeling is the turbulent convection term, for which one can use the following gradient model:

$$- < v''_\alpha | \psi_k > \tilde{P} \cong D_t \partial_\alpha \tilde{P},$$

where D_t is the turbulent diffusion coefficient, which is set to be equal to the eddy viscosity, i.e., the turbulent Schmidt number is equal to one.

The next term needs modeling is the molecular mixing term. A coalescence/dispersion model is used for this term, which has the following general form[6]:

$$\begin{aligned} &-\bar{\rho}\sum_{i=1}^{N}\sum_{j=1}^{N} \partial^2_{\psi_i,\psi_j}(< \epsilon_{ij} | \psi_k > \tilde{P}) \\ &\cong \frac{C_D}{\tau}\int\int \tilde{P}(\psi')\tilde{P}(\psi'')T(\psi|\phi', \psi'')d\psi' d\psi'' - \tilde{P} \\ &\equiv M\,(\tilde{P}) \end{aligned}$$

where T is the transition probability. A new mixing model continuous in time is recently developed by Hsu and Chen[7]. For more detail description of the molecular mixing models, see Refs. 6 and 7.

The modeled pdf equation is then

$$\begin{aligned} &\bar{\rho}\partial_t \tilde{P} + \bar{\rho}\tilde{v}_\alpha \partial_\alpha \tilde{P} + \bar{\rho}\sum_{i=1}^{m} \partial_{\psi_i}\{w_i(\psi_1, \cdots, \psi_m)\tilde{P}\} \\ &= \partial_j(D_t \partial_\alpha \tilde{P}) + M\,(\tilde{P}), \end{aligned} \quad (5)$$

which can be solved using a Monte Carlo simulation.

Numerical Methods

In the present study, a combined finite difference–Monte Carlo solver is developed. For the velocity field, the Navier-Stokes equations and a $k-\epsilon$ turbulence model are solved using a finite difference method; for scalar variables such as the temperature, mass fractions, etc., the pdf evolution equation is solved using a Monte Carlo scheme. The CFD flow solver provides the Monte Carlo solver with the mean velocity and a turbulence time scale τ, where $\tau = k/\epsilon$, and the Monte Carlo solver provides the mean flow solver with the density, $\bar{\rho}$.

The solution of the Navier-Stokes equations

Since the primary concern of the present work is pdf modeling, we choose the simplest possible solver for the N-S equations. The equation is transformed into a general coordinate system using the following general relation:

$$x = \xi$$
$$y = y(\xi, \eta)$$

and

$$\partial_x = \partial_\xi - \frac{y_\xi}{y_\eta}\partial_\eta$$
$$\partial_y = \frac{1}{y_\eta}\partial_\eta$$

The transformed momentum equation for steady flows is

$$\bar{u}\partial_\xi \bar{u} + (\bar{v} - \bar{u}y_\xi)\frac{1}{y_\eta}\partial_\eta \bar{u} = -\frac{1}{\bar{\rho}}\partial_\xi p + \frac{1}{y_\eta}\partial_\eta(\nu_\tau \partial_\eta \bar{u}),$$

where the viscous term involves gradient in the ξ-direction is neglected since we are only interested in shear flows in the present study.

First order upwind difference is used in the ξ-direction so that a marching scheme for steady parabolic flows can be used. To ensure stability, a flux splitting scheme is used in the η-direction.

The solution of the pdf equation

A fractional step Monte Carlo method, as will be described in the following, is used to solve the pdf equation. We first discretize the time derivative in eq. (5) using finite difference: $\partial_t \tilde{P} = (\tilde{P}^{n+1} - \tilde{P}^n)/\Delta t$, then the pdf evolution equation (eq. 5) can be written as

$$\tilde{P}^{n+1} = \{1 - \Delta t\, \tilde{v}_\alpha \partial_\alpha - \Delta t \sum_{i=1}^{m} \partial_{\psi_i} w_i(\psi_1, \cdots, \psi_m) + \Delta t\, \partial_\alpha D_t \partial_\alpha + \Delta t\, M\}\, \tilde{P}^n$$

Using approximate factorization, the above equation is recast as

$$\tilde{P}^{n+1} = (1 - \Delta t \sum_{i=1}^{m} \partial_{\psi_i} w_i(\psi_1, \cdots, \psi_m)) \times (1 + \Delta t M)(1 - \Delta t \bar{\rho}\bar{v}\partial_\alpha + \Delta t \partial_\alpha D_t \partial_\alpha)\, \tilde{P}^n + O(\Delta t)$$
$$\equiv (1 + \Delta t C)(1 + \Delta t M)(1 + \Delta t R)\tilde{P}^n + O(\Delta t),$$

where C denotes the convection operator, m the molecular mixing, and R chemical reactions. With the above expression, we can three processes consecutively:

(1) convection:

$$\tilde{P}^* = (1 + \Delta t C)\tilde{P}^n,$$

(2) molecular mixing:

$$\tilde{P}^{**} = (1 + \Delta t M)\tilde{P}^*,$$

(3) chemical reaction:

$$\tilde{P}^{n+1} = (1 + \Delta t R)\tilde{P}^{**}$$

In the present study, only steady flows are considered, so ∂_t is replaced by ∂_ξ and a marching scheme in the ξ-direction is employed.

In a Monte Carlo simulation, the continuous pdf is replaced by $N \times M$ delta functions,

$$P^*(\psi_1, \psi_2, \cdots, \psi_m; x, y, z, t) = \frac{1}{N}\sum_{n=1}^{N} \delta(\psi_1 - \phi_1^{(n)}(t)) \times \delta(\psi_2 - \phi_2^{(n)}(t)) \cdots \delta(\psi_m - \phi_m^{(n)}(t)),$$

where each product of the m delta functions represents one event of an ensemble of N sample events. An event can be thought of as a fluid particle, and the evolution of P^* entails the movement of the particles in the physical space as well as the phase space (ψ−space). The movement of the particles is, of course, governed by the pdf evolution equation, and is simulated in the following three steps.

Step 1: convection

Replace $\tilde{P}$ by P^* in the pdf evolution equation and transform it into the $\xi - \eta$ coordinate system, the convection process for a steady flow can be written as

$$\bar{\rho}\bar{u}\partial_\xi P^* = -\bar{\rho}(\bar{v} - \bar{u}y_\xi)\frac{1}{y_\eta}\partial_\eta P^* + \frac{1}{y_\eta}\partial_\eta(\bar{\rho} D_t \partial_\eta P^*),$$

Discretizing the above equation using a finite difference scheme, we can write

$$P^*_{i,j} = \alpha P^*_{i-1,j+1} + \beta P^*_{i-1,j} + \gamma P^*_{i-1,j-1}$$

(Here again we used a one sided difference so that a marching scheme could be used.) The above equation states that if we divide the flow field into cells, then the pdf at point (i, j) can be written as a linear combination of the pdf at neighboring points, To simulate this process with a Monte Carlo scheme, we move the sample particles between cells according to the above equation. For instance, the particles of cell (i, j) will be obtained by choosing randomly αN particles form cell $(i-1, j+1)$, βN particles from cell $(i-1, j)$, and γN particles from cell $(i-1, j-1)$. In order for the total number of particles not to change, we require that $\alpha + \beta + \gamma = 1$.

It is worth noting that this method can easily be extended to elliptic flows and applied to general curvilinear coordinate systems.

Step 2: molecular mixing.

The molecular mixing process is simulated by the following binary interaction model:

$$\bar{\rho}\bar{u}\partial_\xi \tilde{P} = \frac{C_D}{\tau}\int\int \tilde{P}(\psi')\tilde{P}(\psi'')T(\psi|\phi',\psi'')d\psi' d\psi'' - \tilde{P}$$

where T is the transition probability. By assigning various functions to T, we would have different mixing models. In the present study, the modified Curl model by Janicka et al. [8] is used. In this model, the transition probability is given as

$$T(\psi|\phi',\psi'') = \begin{cases} \frac{1}{|\psi''-\psi'|} & \text{for } \psi' \le \psi \le \psi'', \\ & \text{or } \psi'' \le \psi \le \psi', \\ 0 & \text{otherwise.} \end{cases}$$

with $C_D = 6.0$.

In the Monte Carlo simulation, the above model is realized in the following manner: Divide the flow domain into small cells, each containing N sample particles. Given a small time interval Δt and a turbulent time scale τ, select randomly N_{mx} pairs of particles, where

$$N_{mx} = 0.5\frac{\Delta t}{C\tau}N,$$

and let a pair, say, m and n, mix as follows

$$\phi_n(t+\Delta t) = A\phi_m(t) + (1-A)\phi_n(t)$$
$$\phi_m(t+\Delta t) = A\phi_n(t) + (1-A)\phi_m(t)$$

where $A = 0.5\xi$, with ξ a random variable uniformly distributed on the interval [0.1]. The remaining $N - 2N_{mx}$ particles remain unchanged:

$$\phi_n(t+\Delta t) = o_n(t)$$

The turbulent time scale is supplied by the finite difference solution of a $k-\epsilon$ turbulence model: $\tau = k/\epsilon$.

This model admits the non-physical jump condition and does not produce the correct long time behavior for decay problems in homogeneous turbulence. A continuous model that predicts the correct long time behavior for turbulence decay problem has been introduced by Hsu and Chen [7]. But as shown in Ref. [7], for practical combustion problems where the long time statistical behavior is not crucial, the modified Curl model gives acceptable results. In the present study, both the modified Curl model and the continuous model have been used.

Step 3: chemical reaction

Chemical reaction is represented in the Monte Carlo simulation by the movement of sample particles in the phase space due to reaction. A sample point with a given composition $\{o_1, \phi_2, \cdots, \phi_m\}$ at time t will acquire new composition at the next moment, and the changing rate is

$$\frac{d\phi_i}{dt} = w_i(\phi_1, \phi_2, \cdots, \phi_m), \quad i = 1, 2, \cdots, M,$$

where w_i is the reaction rate for that specific sample point. If we regard w_i as the convection velocity of the particle in the phase space, the it is clear that the above ODE represent the movement of a sample particle in the phase space.

The various chemistry models considered in this study are presented in the following section.

Chemistry Models for $H_2 - F_2$ Reaction

Finite rate chemistry.

The reaction of $H_2 + F_2 = 2HF$ can be represented by the following two step chain reactions[4]:

$$H_2 + F \longrightarrow^{k_1} HF + H$$
$$H + F_2 \longrightarrow^{k_2} HF + F$$

with

$$k_1 = 2.6 \times 10^{12} T^{0.5} exp\left(\frac{-610}{RT}\right),$$
$$k_2 = 3 \times 10^{9} T^{1.5} exp\left(\frac{-1680}{RT}\right),$$

where T is in K, R in $cal\ mol^{-1}\ K^{-1}$, and k in $cm^3\ mol^{-1}\ sec^{-1}$.

The above expressions only provide the forward reaction rate; the backward reaction rate can be calculated using the equilibrium coefficient:

$$k_b = k_f/k_{eq},$$

and the equilibrium coefficient can be evaluated using Gibbs free energy. Polynomials for Gibbs free energy for various species can be found in Ref. [8]. A numerical experiment shows that the backward reaction rates are much smaller than that of the forward reaction for the two reaction steps described above and can be neglected.

Let C denote the mole concentration; for each sample particle, we need to solve the following set of ODEs:

$$\frac{dC_{H_2}}{dt} = -k_1 C_{H_2} C_F = \omega_1$$
$$\frac{dC_{F_2}}{dt} = -k_2 C_H C_{F_2} = \omega_2$$
$$\frac{dC_H}{dt} = -\omega_1 + \omega_2 = \omega_3$$
$$\frac{dC_F}{dt} = \omega_1 - \omega_2 = \omega_4$$
$$\frac{dC_{HF}}{dt} = -\omega_1 - \omega_2 = \omega_5$$
$$\frac{dh}{dt} = -\sum_{i=1}^{5} h_{f_i}^0 \omega_i$$

where h is the enthalpy and $h_{f_i}^0$ is the heat of formation.

Using n to denote the time level, we found that the following semi-implicit scheme seems to be most stable:

$$C_{H_2}^{n+1} = \frac{C_{H_2}^n}{1 + \Delta t\, k_1 C_F^n}$$

$$C_{F_2}^{n+1} = \frac{C_{F_2}^n}{1 + \Delta t\, k_2 C_H^n}$$

$$C_H^{n+1} = \frac{C_H^n + \Delta t\, k_1 C_{H_2}^n C_F^n}{1 + \Delta t\, k_2 C_H^n}$$

$$C_F^{n+1} = \frac{C_F^n + \Delta t\, k_2 C_{F_2}^n C_H^n}{1 + \Delta t\, k_1 C_{H_2}^n}$$

$$C_{HF}^{n+1} = C_{HF}^n + \Delta t\,(k_1 C_{H_2}^n C_F^n + k_2 C_H^n C_{F_2}^n)$$

The energy equation is solved explicitly. To start the chain reaction 0.00002 mole fraction of F was released into the flowfield initially.

Using the above equations to calculate the reaction in a laminar premixed flame, we found that the time required for this reaction is the order of one microsecond (Figs. 1 and 2). The turbulence time scale in the calculation, $\tau = k/\epsilon$, is the order of one second. Considering this large difference of time scales, it is impractical to use finite rate chemistry in this calculation.

Fast reaction

Since the chemical reaction is very fast compared to the flowfield development and the reverse reactions are negligible, we chose to use the following complete irreversible reaction mechanism. We assume that after molecular mixing, complete reaction is achieved within each particle during the time interval of one marching step in the calculation. The reaction is calculated using the following equations.

For $C_{H_2}^n \geq C_{F_2}^n$:

$$C_{H_2}^{n+1} = C_{H_2}^n - C_{F_2}^n$$
$$C_{F_2}^{n+1} = 0$$
$$C_{HF}^{n+1} = C_{HF}^n + 2C_{F_2}^n$$

For $C_{H_2}^n \leq C_{F_2}^n$:

$$C_{H_2}^{n+1} = 0$$
$$C_{F_2}^{n+1} = C_{F_2}^n - C_{H_2}^n$$
$$C_{HF}^{n+1} = C_{HF}^n + 2C_{H_2}^n$$

The energy equation can be written as

$$\Delta h = -h_{f_{HF}}^0\, \Delta C_{HF} \left(\frac{M_{HF}}{\bar{\rho}}\right),$$

where M_{HF} if the molecular weight of HF.

Since the concentrations of reactants are low, the heat release is low, and the temperature rise is within a few hundred degrees Kelvin. Under these circumstances, the variation of specific heat C_p is negligible, and the temperature can be calculated as

$$T^{n+1} = T^n + \frac{\Delta h}{\overline{C_p}}$$

The error involved in this approximation is less than 5%.

Results and Discussions

Code validation.

Before applied to the hydrogen-fluorine diffusion flames, the computer algorithm is first validated using experimental data for a heated turbulent jet. The non-reacting flow data serves as a check for the convection and molecular mixing process in the pdf solver as well as the $k - \epsilon$ model in the N.-S. solver.

Extensive experimental results for turbulent plane jet have been reported by many authors. Measurements for mean velocity field in a turbulent jet were first reported in the 1930's[9]; turbulent shear stress measurements had been reported more recently[10,11]. To determine the effect of turbulence on mixing, the temperature field of a heated turbulent jet had been studied by several authors. The turbulent jet has a slightly higher temperature than the ambient. Measurements of both the the mean temperature and the rms of the temperature fluctuations were given[12-17].

In the present study of this non-reacting flow case, the temperature field is treated as a conserved scalar and is simulated by the pdf of the temperature; the velocity field and turbulent shear stress are obtained by solving the N.-S. equation and a $k - \epsilon$ turbulence model.

In the finite difference solution of the flowfield, 41 grid points are used across half of the jet width. A symmetry boundary condition is used at the jet centerline. Fig. 3 shows the comparison of the present solution of the mean velocity field with the experimental data, and Fig. 4 presents the numerical solution of the turbulent shear stress as compared to the experimental data. Good agreements between numerical results and experimental data are observed for both the mean velocity field and the turbulent shear stress. The turbulent shear stress is calculated from $- < u'v' > = \nu_\tau \partial u/\partial y$, where $\nu_\tau = C_\mu k_2/\epsilon$. A good prediction of the turbulent shear stress ensures that the turbulent time scale, $\tau = k/\epsilon$, supplied to the Monte Carlo simulation is correct.

For the Monte Carlo simulation of the temperature field, two sample sizes of 1000 and 1500 sample particles per cell are used. The predicted mean temperature and the root mean square (rms) of the temperature variation are presented in Figs. 5 and 6. The results show that both calculations produce fairly good comparisons with the experimental data, which means a sample size of 1000 particles per cell is large enough.

The above validation lends credibility to the N.S. solver as well as the Monte Carlo solver developed in the present study.

$H_2 - F_2$ diffusion flames

The flow conditions for the $H_2 - F_2$ diffusion flames are set according to an experiment performed by Hermanson and Dimotakis (1989). The flame consists two streams. The upper stream contains N_2 and F_2, the flow velocity is $U_1 = 22\,m/s$; the lower stream contains of N_2 and of H_2, with velocity $U_2 = 8.8\,m/s$. In the present study, 6 cases involving various percentage of H_2 and F_2 in the upper and lower stream are considered; the conditions are listed in Table 1, where ΔT_{adj} is the difference between the adiabatic flame temperature and the free stream temperature.

case No.	equivalence ratio	lower stream, mole fraction of H_2	upper stream, mole fraction of F_2	ΔT_{adj}
1	1	0.02	0.02	186
2	1	0.04	0.04	368
3	1	0.06	0.06	554
4	1/4	0.01	0.04	151
5	1/4	0.02	0.08	302
6	1/4	0.04	0.16	600

Table 1. Initial conditions of the flames calculated in the present study.

Fig. 7 shows the calculated temperature rises due to combustion for cases 2 and 5 of Table 1 and the corresponding experimental data. In the figure, δ_T is the shear layer thickness determined by 1% of the temperature rise. ΔT is the actual temperature rise due to combustion. (the two streams have the same temperatures initially,) and ΔT_{adj} is the adiabatic flame temperature assuming complete reaction. The solution for case 2 agrees fairly well with the experimental data for the same case, while the mean temperature is slightly over predicted for case 5. The computation shows the flame center shifts as a result of change in equivalence ratio, which is consistent with the experimental results.

The rms of the temperature variance for cases 2 and 5 are given in Fig. 8. The results show that in a diffusion flame, the temperature variance has two peaks, and the highest values do not coincide with the maximum values of the temperature distribution. The shifting of the flame due to the change of equivalence ratio can also be observed from this figure.

The mass fractions of H_2, F_2 and HF for cases 2 and 5 are presented in FIgs. 9 and 10, respectively. One can see that although a complete reaction chemistry model was used, with the pdf method, results simular to that of a finite rate computation are produced, which is one of the many advantages of the pdf method.

One experimentally established fact is that for the same equivalence ratio, with various mole concentrations of fuel and oxidizer in the flowfield, the normalized temperature stays the same [4,5]. The present calculation confirmed this. Figs. 11 and 12 are the mean temperatures and rms's of the temperature variance for an equivalence ratio of one; three mole concentrations of fuel were considered. One can see that the curves coincide with each other. The same agreements are found for equivalence ratio 1/4 (Figs. 13 and 14).

The pdf distributions for flame temperature at the center and at the outer edge of the flame (for case 2 of Table 1) are plotted in Fig. 15, where the x-axis denotes $(T - < T >)/\sigma$, with $< T >= \tilde{T}$ being the mean temperature and σ the rms. The pdf distributions show that at the center of the flame, the temperature with the highest probability is not far from the adiabatic flame temperature, while at the outer edge of the flame, most of the time one would find a temperature close to that of the free stream temperature. Nonetheless, as a result of external and internal intermittency, low temperature fluid does exist at the center and high temperature fluid the outer edge. Pdf distributions for various species concentration can also be obtained from the solution, but will not be presented here.

Concluding Remarks

A Monte Carlo solution algorithm for the pdf evolution equation has been developed and successfully combined with a finite difference flow solver in the study of turbulent combustion. The algorithm was validated using turbulent mixing data from non-reacting flows. Turbulent diffusion flames of H_2-F_2 were computed using the pdf method, and good agreements between numerical solution and experimental data were observed. The computation identified the change of equivalence ratio as the cause of flame shift, and demonstrated that similarity solution exists for flames with the same equivalence ratio. The present work showed that a grid dependent Monte Carlo scheme can be readily applied to a general curvilinear coordinate system; therefore, it is suitable for realistic reacting flow computations.

Acknowledgement

The author would like to thank Prof. S.B. Pope, Drs. J.-Y. Chen and J.S. Shuen for their helpful discussions. This work is supported by by NASA Lewis Research Center under Contract NAS-25266 with Dr. L.A. Povinelli as program monitor.

References

1. Pope, S.B., " PDF Methods for Turbulent Reactive Flows." Prg. Energy Combust. Sci., 1985, 11, 119-192.

2. Kollmann, W., "The PDF Approach to Turbulent Flow." Theoret. Comput. Fluid Dynamics, 1990, 1, 249-285.

3. Kuznetsov, V.R., and Sabel'nikov, V.A., *Turbulence and Combustion*, Hemisphere Publishing Corp., 1990.

4. Mungal, M.G. and Dimotakis, P.E., "Mixing and Combustion with Low Heat Release in a Turbulent Shear Layer" J. Fluid Mech. 1984, 148, 349-382.
5. Hermanson, J.C. and Dimotakis, P.E., "Effects of Heat Release in a Turbulent, Reacting Shear Layer." J. Fluid Mech. 1989, 199, 333-375.
6. Janicka, J., Kolbe, W., and Kollmann, W., "Closure of the Transport Equation for the Probability Density Function Scalar Field." J Non-Equilib. Thermodyn. 1979, 4, 47.
7. Hsu, A.T. and Chen, J.Y., "A Continuous Mixing Model for PDF Simulations and its Applications to Combusting Shear Flows." 8th Symposium on Turbulent Shear Flows, Munich, Germany, Sept. 9-11, 1991.
8. Gordon, S. and McBride, B.J., "Computer Program for Calculation of Complex Chemical Equilibrium Compositions, Rocket Performance, Incident and Reflected Shocks, and Chapman-Jouguet Detonations." NASA SP-273, March, 1976.
9. Forthmann. E., *Uber Turbulente Strahlausbreitung*, Diss. Gottingen 1933; Schlischting, H., p 747.
10. Bradbury, L.S., "The Structure of Self-Preserving Turbulent Plane Jet," J. Fluid Mech., 1965, 23, 31-64.
11. Gutmark, E. and Wygnanski, I., "The Plane Jet," J. Fluid Mech., 1976, 73, 465-495.
12. Antonia, R.A., Browne, L.W.B., Chambers, A.J., and Rajagopalan, S., "Budget of the Temperature Variance in a Turbulent Plane Jet." Int. J. Heat Mass Transfer, 1983, 26-1, 41-48.
13. Ashir, J. and Uberoi, M.S., "Experiments on Turbulent Structure and Heat Transfer in a Two Dimensional Jet." Physics of FLuids, 1975, 18-4, 405-410.
14. Browne, L.W.B., Antonia, R.A., and Chembers, A.J., "The Interaction Region of a Turbulent Plane Jet." J. Fluid Mech., 1984, 149, 355-373.
15. Jenkins, P.E. and Goldschmidt, V.W., "Mean Temperature and Velocity in a Plane Turbulent Jet," ASME J. Fluids Eng., 1973, 95, 581-584.
16. Uberoi, M.S. and Singh, P.I., "Turbulent Mixing in a Two-Dimensional jet," Physics of Fluids, 1975, 18-7, 764-769.
17. Bashir, J. and Uberoi, M.S., "Experiments on Turbulent Structure and Heat Transfer in a Two Dimensional Jet." Physics of Fluids, 1975, 14.4, 405-410.

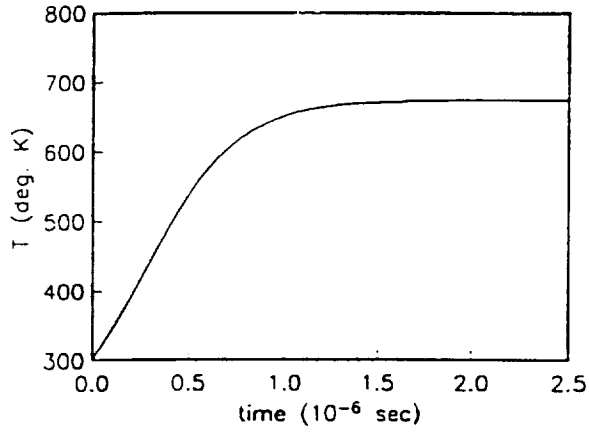

Figure 1. Temperature rise in a premixed laminar H_2–F_2 flame.

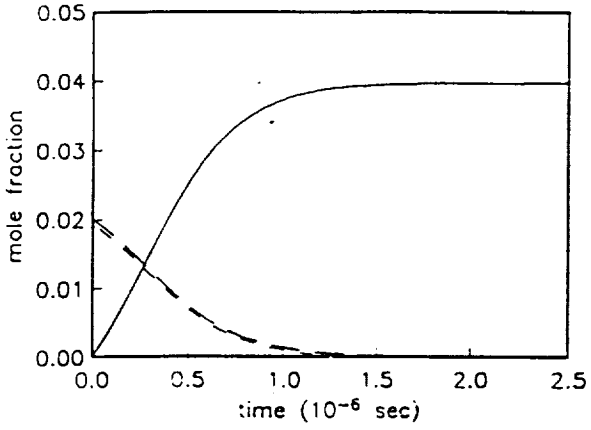

Figure 2. Changes of mass fractions in a premixed laminar H_2–F_2 flame. - - - H_2, – – – F_2, — HF.

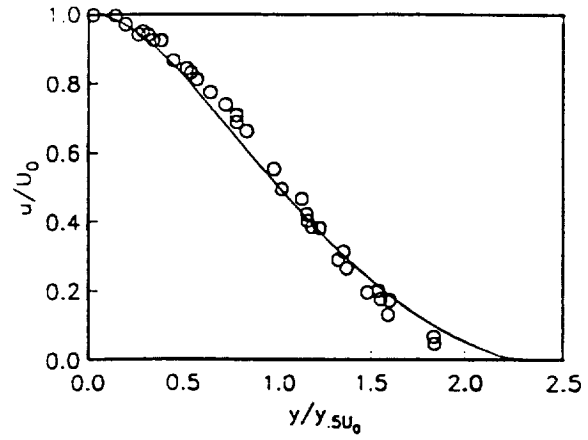

Figure 3. Mean velocity distribution in a 2D turbulent jet. o Ref [9], — Present calculation.

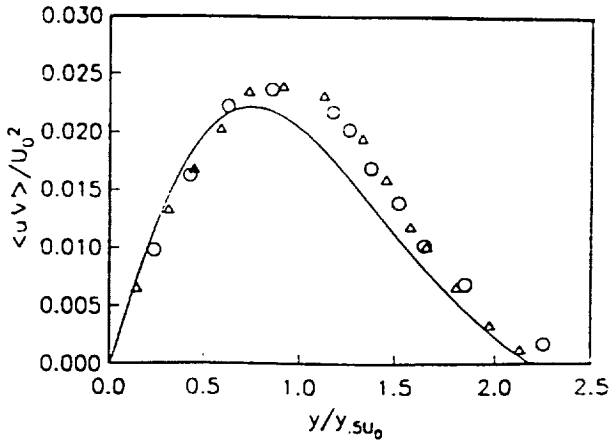

Figure 4. Turbulent shear stress in a 2D turbulent jet. o Ref [10], △ Ref [11], — Present calculation.

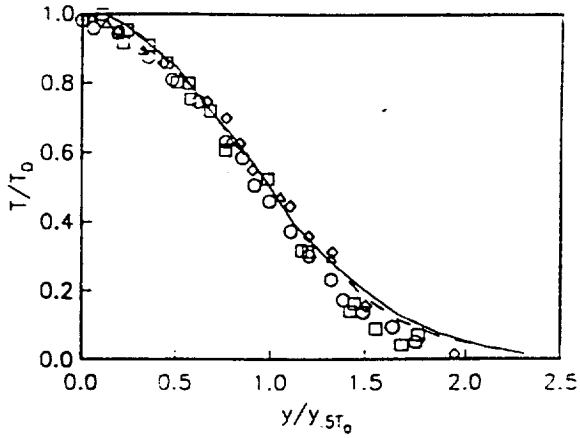

Figure 5. Mean temperature in heated plane jet. △ Ref [14], ⊓ Ref [17], o Ref [16] o Ref [15]. — pdf solution, 1500 particles per cell; - - - pdf solution. 1000 particles per cell.

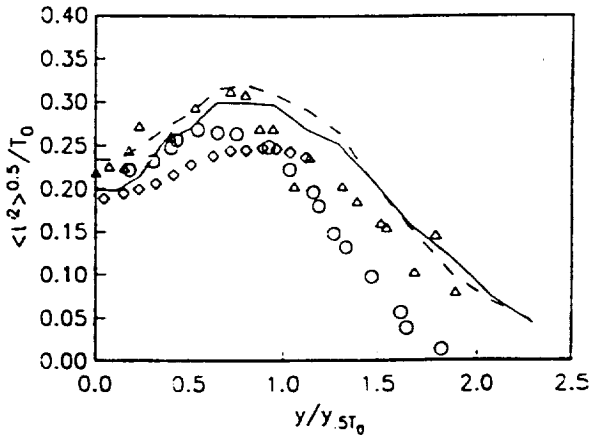

Figure 6. RMS of temperature variance in heated plane jet. o Ref [12], o Ref [17], △ Ref [16], — pdf solution. 1500 particles per cell; - - - pdf solution. 1000 particles per cell.

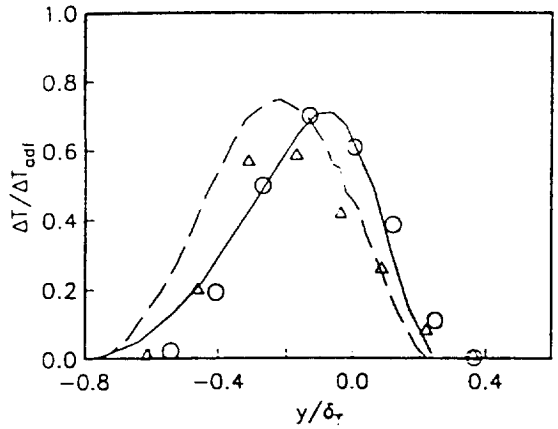

Figure 7. Mean temperature rises in H_2–F_2 diffusion flames. Case 2 (refer to Table 1): o Ref [5], — present; Case 5: △ Ref [5], - - - present.

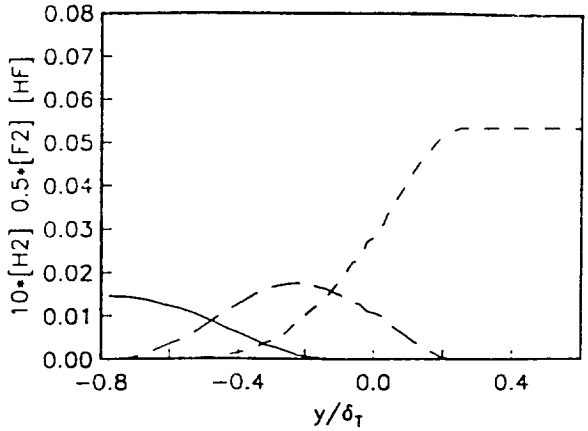

Figure 10. Mass fraction distributions in an H_2–F_2 flame, case 5, equivalence ratio 1/4. — H_2, - - - F_2, – – HF.

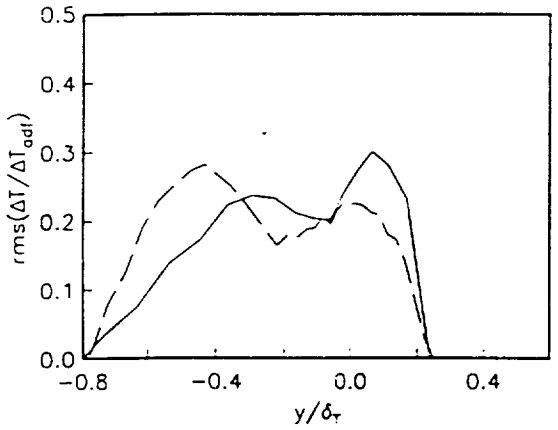

Figure 8. RMS of Temperature variance in H_2–F_2 diffusion flames. — equivalence ratio 1 (case 2, Table 1). - - - equivalence ratio 1/4 (case 5).

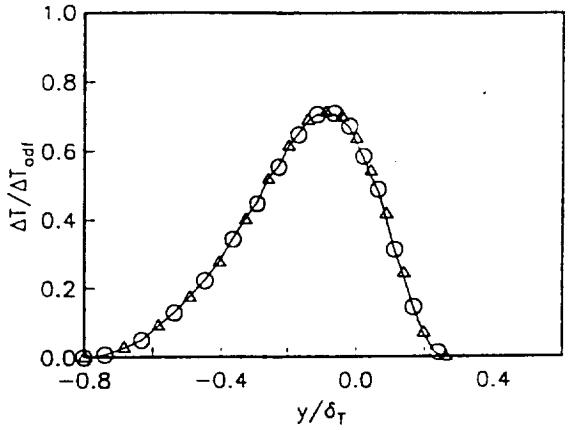

Figure 11. Mean temperature rises in H_2–F_2 flames, equivalence ratio 1. Referring to Table 1: — case 1, o case 2, △ case 3.

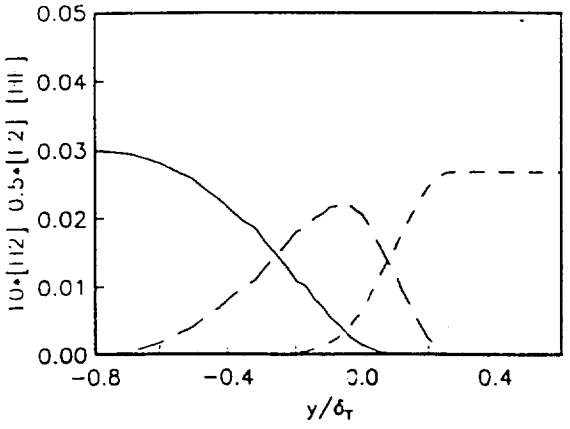

Figure 9. Mass fraction distributions in an H_2–F_2 flame, case 2, equivalence ratio 1. — H_2, - - - F_2, – – HF.

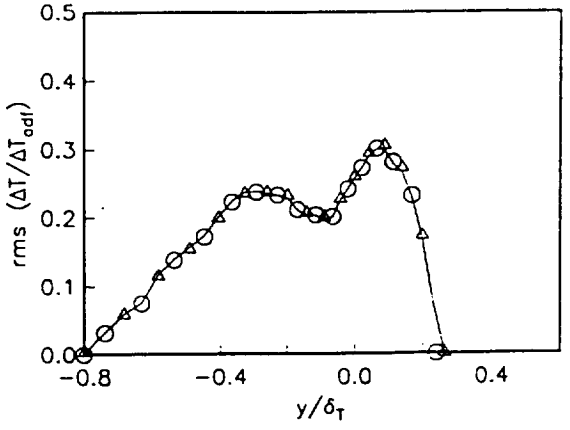

Figure 12. RMS of temperature variance in H_2–F_2 flames, equivalence ratio 1. Referring to Table 1: — case 1, o case 2, △ case 3.

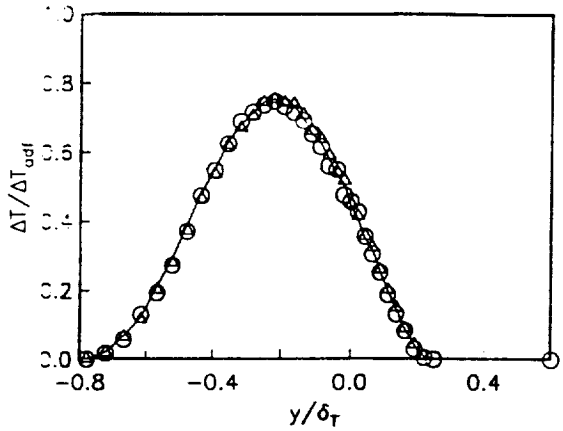

Figure 13. Mean temperature rises in H_2–F_2 flames, equivalence ratio 1/4. Referring to Table 1: — case 4, o case 5, △ case 6.

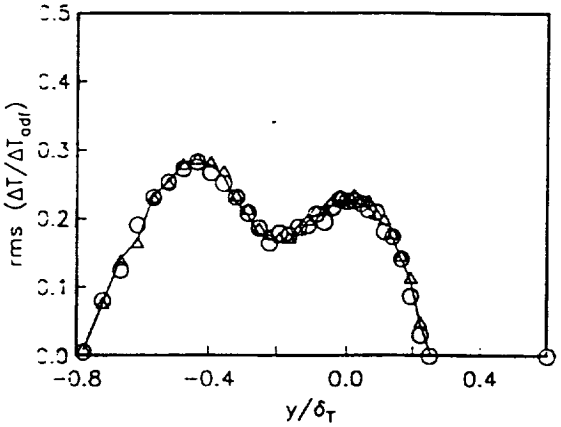

Figure 14. RMS of temperature variance in H_2–F_2 flames, equivalence ratio 1/4. Referring to Table 1: — case 4, o case 5, △ case 6.

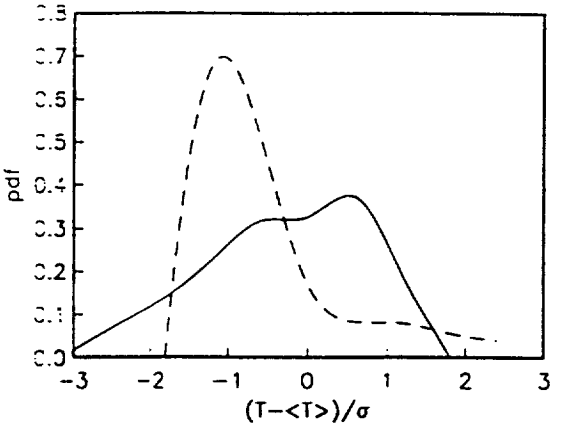

Figure 15. Probability density function distributions in an H_2–F_2 flame (case 2). — pdf at the center of the flame, - - - pdf at the out edge of the flame.